

Probing the transition from an uncoupled to a strong near-field coupled regime between bright and dark mode resonators in metasurfaces

Ranjan Singh,^{1,a)} Ibraheem Al-Naib,² Dibakar Roy Chowdhury,³ Longqing Cong,¹ Carsten Rockstuhl,⁴ and Weili Zhang⁵

¹Centre for Disruptive Photonic Technologies, Division of Physics and Applied Physics, School of Physical and Mathematical Sciences, Nanyang Technological University, Singapore, Singapore 637371

²Department of Physics, Engineering Physics and Astronomy, Queen's University, Kingston, Ontario K7L 3N6, Canada

³Center for Sustainable Energy Systems, College of Engineering and Computer Science, Australian National University, Canberra 0200, Australia

⁴Institute of Theoretical Solid State Theory, Institute of Nanotechnology, Karlsruhe Institute of Technology, Karlsruhe, Germany

⁵School of Electrical Engineering and Computer Science, Oklahoma State University, Stillwater, Oklahoma 87074, USA

(Received 18 June 2014; accepted 1 August 2014; published online 27 August 2014)

The coupling of multiple plasmonic resonators that sustain bright or dark modes provide intriguing spectral signatures. However, probing the onset of coupling effects while engaging the resonators with an increasing proximity has not yet been studied experimentally in detail. Nevertheless, this is of utmost importance to bridge the phenomenological understanding with the peculiarities of real-world-samples. Here, we take advantage of the ability to control spatial dimensions of THz metasurfaces deep in the sub-wavelength domain to study different regimes that occur while coupling split-ring-resonators that sustain a bright and a dark mode with increasing strength. We identify the length scales at which the resonators are uncoupled and then enter the regimes of weak, moderate, and strong coupling. It is shown that a strong coupling takes place only at distances smaller than one hundredth of the resonance wavelength. Understanding the features that emerge from such hybridization is important to take advantage of fundamental effects in metamaterials such as classical analogs of electromagnetically induced transparency, lasing spaser, near-field manipulation, and sensing with dark mode resonances. © 2014 AIP Publishing LLC.

[<http://dx.doi.org/10.1063/1.4893726>]

Metasurfaces are thin films of artificially structured materials with unusual but highly beneficial electromagnetic properties.^{1,2} These properties are provided at user-defined frequencies while relying on periodically or amorphously arranged unit cells with critical dimensions smaller than the operational wavelength.² While relying on unit cells, usually dubbed as meta-atoms that do provide an electromagnetic response that deviates from an ordinary electric dipole, properties inaccessible with naturally occurring materials fall within reach.^{3–6} A canonical meta-atom in this stream of research is the split-ring-resonator (SRR) but many others can be considered as well. The key to tailor all anticipated properties upon demand is the ability to control the design and the geometrical detail of these meta-atoms with high precision.

However, spectral properties with an even larger sophistication fall within reach while considering unit cells that consist of multiple coupled meta-atoms. These advanced unit cells are called metamolecules in analogy to metaatoms. A basic categorization of metamolecules can be made while considering designs for which the coupling is enforced by electromagnetic fields.^{7–15} Recently, there have been several works where near-field coupling among metaatoms was investigated that sustain a bright and a dark mode.^{8–10,14,15} The term bright and dark mode refers here to the ability to

excite a particular resonance with the given polarization of the illumination if the individual metaatoms that form the metamolecule are uncoupled. These laterally coupled resonators lead to fascinating effects such as classical analogs of electromagnetically induced transparency and slow light.⁹ However, the critical length-scales at which the onset of near-field coupling between bright and dark mode occurs has not been extensively studied; but in most cases only a single unit cell has been considered. This, however, is insufficient if a basic phenomenological description of the effects shall be linked to real-world samples. Thus, it is necessary to fully understand the near-field interactions effects of the two resonators in order to develop an understanding of how strong the coupling actually is. Moreover, being in the position to set-up on purpose, a weak or a strong coupling regime will allow in the near future to transpose much more effects that concern the light-matter interaction at the quantum level to plasmonic analogies.

Therefore, in this work, we bridge this gap of physics and study the typical length scales at which the near-field coupling between bright and dark mode resonators occurs. This shall lead to different levels of splitting of the involved resonance. To this end, we rely on laterally coupled, orthogonally twisted resonators in a unit cell of a planar terahertz metasurface and consider their fundamental (*LC*) resonance. Thus far, there are reports of different strategies in metamaterial research to achieve electromagnetic coupling.^{6–26} The

^{a)}Email: ranjans@ntu.edu.sg

near-field coupled metamaterials can involve electric coupling,^{7,12,16} magnetic,^{8,10,14,17,19–26} as well as both electric and magnetic coupling.^{9,11–13} Resonance mode splitting in magnetically coupled system based on bright and dark resonators is demonstrated earlier in the context of weakly inductive and strongly conductively coupled cases.^{8–10,14,15}

The unit cell consists of two orthogonally twisted split ring resonators placed beside each other with varying inter-SRR distance d (see Fig. 1). According to the polarization of the incident excitation beam, we term the resonator that is directly excited by the incident electromagnetic field as bright. On the contrary, the resonator that can only be excited by the near-field of the bright resonator is called the dark resonator. Therefore, the SRR with the split gap aligned parallel to the incident electric field of the terahertz beam is termed as bright resonator, since its fundamental LC resonance can be excited. The neighboring orthogonally twisted resonator is the dark one as its fundamental LC resonance is inaccessible with the same polarization of the incident terahertz field. These neighboring bright and dark mode resonators within the unit cell are coupled through their electromagnetic near-fields. With large inter resonator distances, the coupling between the resonators is weak, leading to very small or no split of the fundamental resonance. In other words, the fundamental resonance of the dark resonator cannot be excited. As the resonators are brought closer, the near-field interaction increases, leading to the excitation of the fundamental resonance in the dark resonator. Since the fundamental LC resonance of the SRR is usually associated with a magnetic dipolar response, we consider the interaction as predominantly magnetic. However, it is worth to stress that the fundamental resonance is not only just characterized by the magnetic dipole moment (normal to the plane of the SRR) but also by an electric dipole moment (in the plane of the SRR and parallel to its base). Both of these moments generate electromagnetic fields, which can couple to the eigen modes sustained by the twisted SRR. The orthogonality of the modes is lifted and the coupling eventually is only possible by the slight asymmetry in the sample induced by the gap that is engraved into only one of the two bases of the SRR.

Numerical simulations clearly indicate a significant enhancement of induced electric field lines inside the dark resonator split gap along with the induction of circular surface currents in the dark resonator metallic arms. This fact confirms the excitation of the LC resonance mode within the dark resonator. We will categorize four regimes of

interactions, depending on the inter resonator distances and the corresponding spectral splitting of the fundamental resonance. They are named as the *no coupling* regime, the *weak coupling* regime, the *moderate coupling* regime, and the *strong coupling* regime. These regimes are defined according to the spectral response of the coupled system when compared to that of the isolated bright resonator. If the spectral response of the coupled system largely resembles that of an isolated bright SRR, it is called uncoupled. If the shape and the strength of the individual resonances of the bright SRR starts to deviate but remains to be an isolated resonance, it is called the weak coupling regime. Moreover, if a minor spectral trace of a coupling tends to be visible in terms of a weak splitting, the regime is called the moderate coupling regime. And eventually, whenever the splitting is clearly visible, the regime is called the strong coupling regime. This classification should eventually be universal to all planar metamaterials where unit cells consist of multiple metaatoms.

The samples were fabricated on a $640\ \mu\text{m}$ thick n-type silicon substrate through typical photo-lithography procedure and the SRRs were formed by using $200\ \text{nm}$ thick aluminum as shown in Fig. 1. Geometrical descriptions of the fabricated samples along with the optical microscope image are shown in Fig. 1(a). The measurements were carried out using a typical $8f$ confocal photo-conductive based terahertz time-domain spectroscopy (THz-TDS) system. The polarization of the incident terahertz electric field is aligned parallel to the gap-bearing arm of the bright SRR.

The transmission spectra of five different sets of coupled bright and dark resonator based metamaterial samples were measured as shown in Fig. 2(a), with separations of $d = 4\ \mu\text{m}$, $3\ \mu\text{m}$, $2\ \mu\text{m}$, $1\ \mu\text{m}$, and $0\ \mu\text{m}$, respectively. In the case of the sample with $0\ \mu\text{m}$ separation between the bright and dark resonators in the unit cell, the fundamental LC resonance has the maximum splitting and the split resonances appear at $0.437\ \text{THz}$ and $0.584\ \text{THz}$. For $1\ \mu\text{m}$ inter resonator separation, split resonances appear at $0.456\ \text{THz}$ and $0.548\ \text{THz}$. Similarly, for inter resonator separation of $2\ \mu\text{m}$ ($3\ \mu\text{m}$), the split resonances occur at $0.468\ \text{THz}$ ($0.478\ \text{THz}$) and $0.546\ \text{THz}$ ($0.544\ \text{THz}$), respectively. When resonators are separated by $4\ \mu\text{m}$, higher frequency split resonance is observed at $0.535\ \text{THz}$. The split resonance at lower frequency is not seen in the experiment due to the limited resolution ($58.8\ \text{GHz}$) of the terahertz measurement set-up. The experimental transmission data have been further validated through finite integration technique numerical simulations using commercially available software, CST Microwave Studio as shown in Fig. 2(b). In simulations, the metal conductivity value is $3.56 \times 10^7\ \text{S/m}$ and substrate permittivity is 11.68 with loss tangent of 0.015 . Minor differences between measurements and simulations could be attributed to the mismatch in dimensions of the actual fabricated sample and the simulated structure.

Figure 3(a) shows the LC resonance of a single bright resonator in the unit cell of the metasurface array, which we have chosen to highlight the nature of the resonance without any involvement of dark mode coupling in the unit cell (λ_{LC}). We further observe in Fig. 3(b) that when the separation between the bright and dark modes is larger ($>15\ \mu\text{m} \sim \lambda_{LC}/40$), we only see the bright mode LC resonance

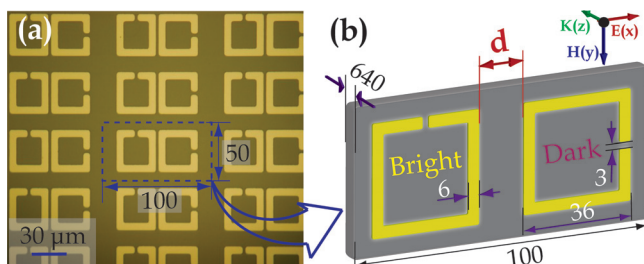


FIG. 1. (a) Image of the fabricated sample array with inter resonator distance $d = 2\ \mu\text{m}$. (b) Schematic description of the bright and dark unit cell with varying “ d .” All dimensions are given in micron.

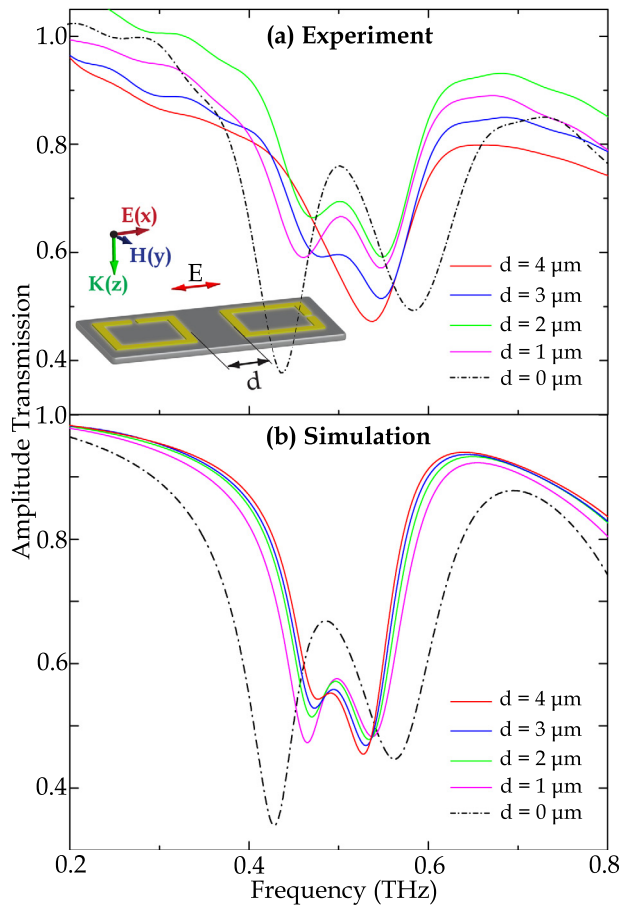


FIG. 2. (a) Measured and (b) simulated amplitude transmission for different d values.

without any signature of the dark mode excitation. These distances could be defined as the uncoupled regime. Only at distances $< 15 \mu\text{m}$, we notice changes in the line shape of the bright mode that marks the onset of the dark mode excitation. Thus, we define the region between $10 \mu\text{m}$ and $15 \mu\text{m}$ as the weakly coupled regime. At distances between $5 \mu\text{m}$ and $10 \mu\text{m}$, we observe a minor split in the LC resonance, thus we address this region as moderately coupled. The mode splitting becomes very clear at distances $< 5 \mu\text{m}$ ($\lambda_{LC}/120$). Thus, we define this length scale as the strong near-field coupling zone. In the extreme near-field coupling regime at sub-micron distances ($d < 1 \mu\text{m} \sim \lambda_{LC}/600$), the coupling between the bright and dark mode tends to be very strong and eventually becomes the strongest for distance of $d = 0 \mu\text{m}$, where the resonators touch and become conductively coupled as compared in Fig. 3(c). We have summarized the different coupling regimes in Fig. 4, where the central horizontal line at 0.51 THz denotes the LC resonance of a bright single resonator and the dots above and below the central line shows the split resonances of a coupled bright and dark mode resonators. For the sub-micron proximity of the interacting bright and dark resonators, the magnetic coupling is strongest leading to the maximum separation between the split resonances.

The LC resonance mode originates in the coupled structure from the resonant electric currents oscillating around the circumference of the bright SRR resonator.^{27–29} The

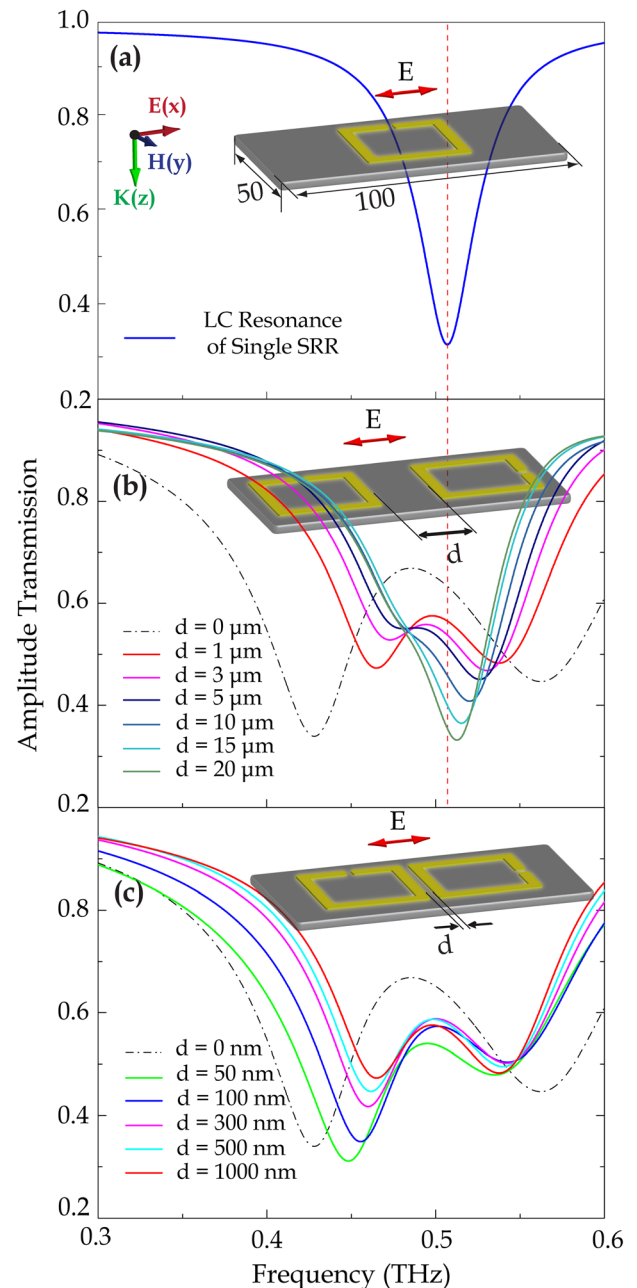


FIG. 3. Simulated (a) LC resonance of a single SRR, (b) coupled bright and dark SRRs with different inter SRR separations, and (c) coupled SRRs with sub-micron separations.

oscillating current is induced by the incident electric field of the probing terahertz beam aligned parallel to the SRR gap arm of the bright resonator. The LC resonance is first excited in the bright SRR. The electromagnetic field generated around the bright SRR then excites the LC mode in the orthogonally twisted neighbouring dark SRR through the near-field inductive coupling. After the circular currents are set up in both the neighbouring resonators within the unit cell, the resonators couple to each other through their self-consistent electromagnetic field, leading to resonance mode hybridization³⁰ which is reflected in clear splitting of the fundamental resonances. The separation between the split resonances indicates the extent of near-field interaction or coupling in between the resonators. In this coupled system, the LC resonance splits into two modes in which induced

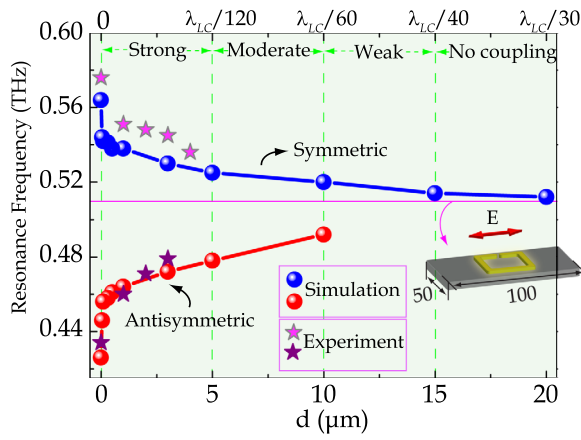


FIG. 4. The experimental and simulated split resonance dip frequencies are plotted versus the bright and dark SRR separation distances. The central horizontal line at 0.51 THz shows the intrinsic LC resonance (λ_{LC}) of the bright SRR.

surface current densities oscillate out of phase at the lower asymmetric resonance frequency and in phase at the symmetric higher resonance frequency.^{8,10}

We have further simulated the surface current and electric field profiles developed across the split ring resonators for several inter resonator separations at the lower resonance dip. In Fig. 5, the surface currents and electric fields are shown for relatively larger separations ranging from $d = 15 \mu\text{m}$ to $d = 1 \mu\text{m}$. Similarly, Fig. 6 demonstrates the profiles for the tightly coupled sub-micron regimes ranging from $d = 0.5 \mu\text{m}$ to $d = 0 \mu\text{m}$. When the resonators are significantly away with inter resonator distances of $15 \mu\text{m}$ or $8 \mu\text{m}$, the surface current in the bright resonator shows a clear LC behaviour as shown in Figs. 5(a) and 5(c).

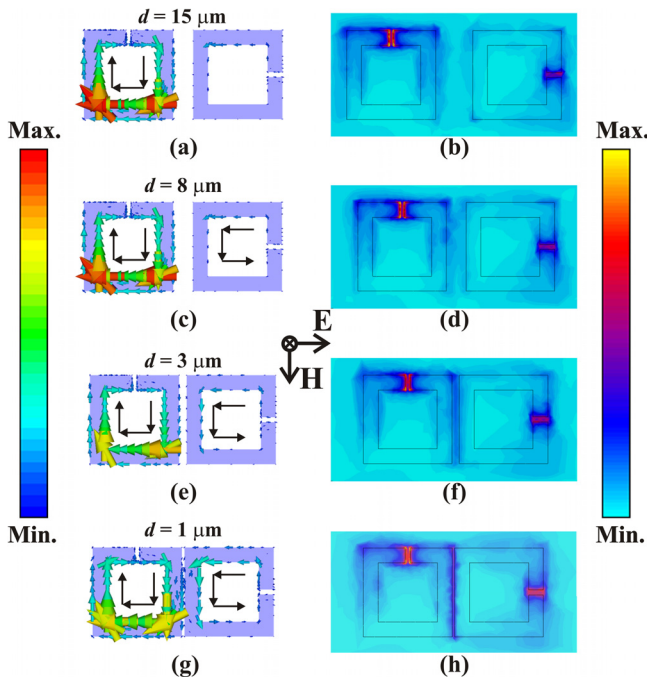


FIG. 5. Simulated surface current are shown in the panels (a), (c), (e), and (g) at different distances between the bright and dark resonators. Panels (b), (d), (f), and (h) depict the corresponding electric field. The simulations were carried out at lower resonance frequencies.

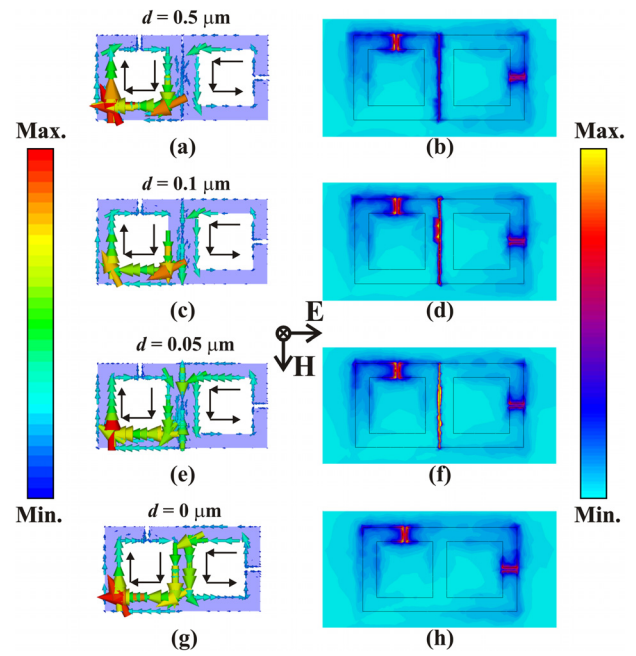


FIG. 6. The surface current distributions are shown in (a), (c), (e), and (g) and the corresponding electric fields (b), (d), (f), and (h) are shown when the bright and dark SRRs are operating in the strongly coupled regime at different separations. The simulations were carried out at lower resonance frequencies.

However, there is almost no sign of induced circular current in the dark resonator. The induced electric field distribution is indicated for these two inter resonator separations in Figs. 5(b) and 5(d), respectively. Although strong electric field is induced in the bright resonator but there is hardly any induced electric field in the dark resonator split gap (Figs. 5(b) and 5(d)). In case of inter resonator separation of $d = 3 \mu\text{m}$, a weak surface current is developed across the dark resonator (Fig. 5(e)) along with minor development of electric fields inside the dark resonator split gap (Fig. 5(f)). With the inter resonator distance reducing further to $1 \mu\text{m}$, stronger surface current develops (Fig. 5(g)) in the dark resonator with stronger electric field across the dark resonator split gap (Fig. 5(h)). As the resonators are brought further closer with inter resonator separation at the sub-micron length scales, the surface current induced in the dark resonator increases steadily, as it is evident from Figs. 6(a), 6(c), 6(e), and 6(g). In Fig. 6(e), we observe an anomalous antiparallel surface current between the closest arms of the two SRRs due to extreme near-field coupling case at a physical separation case of $d = 50 \text{ nm}$ only at one particular phase instance. At other values of phase instances, we observe parallel currents in this case. For the corresponding strongly coupled cases, the electric field strength inside the dark resonator split gap undergoes gradual enhancement as shown in Figs. 6(b), 6(d), 6(f), and 6(h). When both the resonators are touching, the inter resonator coupling is the strongest which reflects in maximum strength of the surface current and intense electric fields in the dark resonator.

We have observed the onset and subsequent strengthening of the magnetic coupling between bright and dark mode resonators in metasurfaces where the constituent SRRs are near-field coupled. Our observations indicate that for resonators separated by large distances ($d > \lambda_{LC}/40$), the coupling

is absent; therefore, fundamental resonance mode in dark resonator cannot be excited. As the inter resonator separation between the two SRRs decreases gradually, the fundamental resonance mode of the dark resonator is excited through *weak* ($\lambda_{LC}/60 < d < \lambda_{LC}/40$), *moderate* ($\lambda_{LC}/120 < d < \lambda_{LC}/60$) and *strong* ($d < \lambda_{LC}/120$) coupling. We expect this coupling effect in metamolecules to be universal across all electromagnetic domains. The near-field coupling in metasurfaces would continue to play a significant role in design of lasing spasers, high quality factor sensors, and slow light devices based on classical analogs of electromagnetically induced transparency.

The authors acknowledge funding support from NTU start up grant and United States NSF grant.

- ¹N. Yu and F. Capasso, *Nat. Mater.* **13**, 139 (2014).
- ²J. B. Pendry, A. Holden, D. Robbins, and W. Stewart, *IEEE Trans. Microwave Theory Tech.* **47**, 2075 (1999).
- ³R. A. Shelby, D. R. Smith, and S. Schultz, *Science* **292**, 77 (2001).
- ⁴T. J. Yen, W. J. Padilla, N. Fang, D. C. Vier, D. R. Smith, J. B. Pendry, D. N. Basov, and X. Zhang, *Science* **303**, 1494 (2004).
- ⁵W. Padilla, A. J. Taylor, C. Highstrete, M. Lee, and R. D. Averitt, *Phys. Rev. Lett.* **96**, 107401 (2006).
- ⁶C. M. Soukoulis, S. Linden, and M. Wegener, *Science* **315**, 47 (2007).
- ⁷R. S. Penciu, K. Aydin, M. Kafesaki, Th. Koschny, E. Ozbay, E. N. Economou, and C. M. Soukoulis, *Opt. Express* **16**, 18131 (2008).
- ⁸N. Liu, S. Kaiser, and H. Giessen, *Adv. Mater.* **20**, 4521 (2008).
- ⁹S. Zhang, D. A. Genov, Y. Wang, M. Liu, and X. Zhang, *Phys. Rev. Lett.* **101**, 047401 (2008).
- ¹⁰R. Singh, C. Rockstuhl, F. Lederer, and W. Zhang, *Phys. Rev. B* **79**, 085111 (2009).
- ¹¹O. Sydoruk, E. Tarartschuk, E. Shamonina, and L. Solymer, *J. Appl. Phys.* **105**, 014903 (2009).
- ¹²I. Sersic, M. Frimmer, E. Verhagen, and A. F. Koenderink, *Phys. Rev. Lett.* **103**, 213902 (2009).
- ¹³N. Liu and H. Giessen, *Angew. Chem., Int. Ed.* **49**, 9838 (2010).
- ¹⁴D. R. Chowdhury, R. Singh, A. J. Taylor, H.-T. Chen, and A. K. Azad, *Appl. Phys. Lett.* **102**, 011122 (2013).
- ¹⁵Y. Yang, R. Huang, L. Cong, Z. Zhu, J. Gu, Z. Tian, R. Singh, S. Zhang, J. Han, and W. Zhang, *Appl. Phys. Lett.* **98**, 121114 (2011).
- ¹⁶D. R. Chowdhury, R. Singh, M. Reiten, J. Zhou, A. J. Taylor, and J. F. O'Hara, *Opt. Express* **19**, 10679 (2011).
- ¹⁷J. Wallauer, A. Bitzer, S. Waselikowski, and M. Walther, *Opt. Express* **19**, 17283 (2011).
- ¹⁸K. Aydin, I. M. Pryce, and H. A. Atwater, *Opt. Express* **18**, 13407 (2010).
- ¹⁹V. A. Fedotov, N. Papisimakis, E. Plum, A. Bitzer, M. Walther, P. Kuo, and D. P. Tsai, *Phys. Rev. Lett.* **104**, 223901 (2010).
- ²⁰R. Singh, C. Rockstuhl, and W. Zhang, *Appl. Phys. Lett.* **97**, 241108 (2010).
- ²¹D. A. Powell, M. Lapine, M. V. Gorkunov, I. V. Shadrivov, and Y. S. Kivshar, *Phys. Rev. B* **82**, 155128 (2010).
- ²²R. Singh, C. Rockstuhl, F. Lederer, and W. Zhang, *Appl. Phys. Lett.* **94**, 021116 (2009).
- ²³W. Cao, R. Singh, C. Zhang, J. Han, M. Tonouchi, and W. Zhang, *Appl. Phys. Lett.* **103**, 101106 (2013).
- ²⁴I. Al-Naib, C. Jansen, R. Singh, M. Walther, and M. Koch, *IEEE Trans. THz Sci. Technol.* **3**, 772–782 (2013).
- ²⁵I. Al-Naib, E. Hebestreit, C. Rockstuhl, F. Lederer, D. Christodoulides, T. Ozaki, and R. Morandotti, *Phys. Rev. Lett.* **112**, 183903 (2014).
- ²⁶D. R. Chowdhury, A. K. Azad, W. Zhang, and R. Singh, *IEEE Trans. THz Sci. Technol.* **3**, 783 (2013).
- ²⁷I. Al-Naib, R. Singh, C. Rockstuhl, F. Lederer, S. Delprat, D. Rocheleau, M. Chaker, T. Ozaki, and R. Morandotti, *Appl. Phys. Lett.* **101**, 071108 (2012).
- ²⁸R. Singh, I. Al-Naib, W. Cao, C. Rockstuhl, M. Koch, and W. Zhang, *IEEE Trans. Terahertz Sci. Technol.* **3**(6), 820 (2013).
- ²⁹R. Singh, W. Cao, I. Al-Naib, L. Cong, W. Withayachumnankul, and W. Zhang, pre-print [arXiv:1406.7194](https://arxiv.org/abs/1406.7194) [physics.optics] (2014).
- ³⁰E. Prodan, C. Radloff, N. J. Halas, and P. Nordlander, *Science* **302**, 419 (2003).